Reliability analysis of the influence of seepage on levee stability

Robert Lanzafame PhD Lecturer, Department of Hydraulic Engineering, Technical University of Delft, Delft, the Netherlands (corresponding author: r.c.lanzafame@tudelft.nl)

Nicholas Sitar PhD Professor, Department of Civil and Environmental Engineering, University of California–Berkeley, Berkeley, CA, USA

Abstract

Reliability analysis is used to evaluate the probability of failure of a flood defence embankment subject to a blanket layer foundation condition, where high seepage forces increase the likelihood of internal erosion and slope failure. The stochastic effect of hydraulic conductivity and blanket layer thickness, in addition to soil shear strength properties, is considered for the underseepage and slope stability failure modes using the first-order reliability method. The blanket layer thickness controls the factor of safety (F) and reliability, followed by the unit weight of the blanket layer. Despite variation over orders of magnitude, hydraulic conductivity is less important than and comparable to the effect of soil shear strength parameters. Aleatory uncertainty is evaluated using fragility curves and a confidence interval on the expected value of F (stochastic F). Uncertainty in probability distribution parameters allows quantification of a subset of epistemic uncertainty and is used to construct confidence intervals for fragility.

Notation

c'	effective stress soil cohesion: kPa
F	factor of safety for underseepage (F_{us}) and slope stability (F_{ss})
$F(\boldsymbol{x})$	factor of safety as a function of stochastic variables, $\boldsymbol{x}$
H_E	embankment height: m
h_B	net total hydraulic head, measured across the blanket: m
i	hydraulic gradient across the blanket, $i = h_B/z_B$
K	hydraulic conductivity: m/s
K_r	hydraulic conductivity ratio, measured between aquifer (K_a) and blanket (K_b)
$P[\cdot]$	unknown cumulative distribution function (CDF) of $F(\boldsymbol{x})$
p	probability for the limit state, $F(\boldsymbol{x}) \leq 1{\cdot}0$, referred to as failure probability
$\boldsymbol{x}$	vector of random variables included in a stochastic analysis
x_i	random variable i in a first-order reliability method (FORM) analysis
z_1, z_2	upper and lower limits of the truncated normal distribution
$\boldsymbol{\alpha}$	unit normal vector to the half-space approximation
α_i	importance measure (from FORM) for random variable i
β	reliability index, related to failure probability by $p = \Phi(-\beta)$
γ	saturated soil unit weight: kN/m^3
λ, ζ	parameters of the lognormal distribution
μ_{FS}	stochastic (mean) estimate of the factor of safety (aleatory), with confidence interval σ_{FS}
σ_β	confidence bound (epistemic) on fragility
ϕ'	effective stress soil friction angle: °

Introduction

Earthen embankments, or levees, are flood defence structures constructed to protect an area of land during a period of high water. In contrast to dams, levees are long structures than retain high water only occasionally, during floods. Historically, levee design in the USA has been based on minimum safety factors specified for various modes of failure (DWR, 2012; USACE, 2000). Since first established in the mid-nineteenth century, most levees in California have been continually enlarged and lengthened, responding to changing land use and changing regulatory environment (Kelley, 1998; Seed *et al.*, 2012). Due to being located on floodplains and being close to active stream channels, the foundation soils underlying a levee are often unconsolidated floodplain deposits ranging in size from cobbles and gravel to clay, which can change character dramatically over a short distance (e.g. DWR, 2012). While the most commonly reported mechanism of failure is overtopping, other common failure mechanisms include piping – that is, internal erosion caused by seepage through or under the levee – and, less

frequently, slope failures induced by seepage through the levee (e.g. ASCE, 2010). In addition to these common modes of failure, there are many other conditions that can lead to failure or influence other failure modes, such as penetrations (e.g. pipelines), mammal burrows, current erosion, wave erosion and/or vegetation (DWR, 2012). During periods of high water, there is a hydraulic head difference between the waterside (i.e. river channel) and landside of a levee, inducing flow through the embankment and the foundation (e.g. Cedergren, 1997; Harr, 2012). The resulting seepage forces negatively influence the stability of the slope by adding to the driving force and reducing soil strength, respectively (e.g. Duncan and Wright, 2005; Holtz and Kovacs, 1981).

Given the extent of the levee systems and the complexity of the interaction between the different potential modes of failure, stochastic methods are increasingly being applied in the context of risk analysis to assess potential for failure and to prioritise repairs and modifications. To communicate risk effectively, the probability of occurrence of a failure mode (e.g. underseepage or slope stability) must capture the uncertainty associated with a failure mechanism model and the associated physical parameters (Phoon *et al*., 2003). In this context, it is necessary to distinguish two sources of uncertainty: (*a*) aleatory uncertainty is associated with the natural variability of a phenomenon or physical property, whereas (*b*) epistemic uncertainty is associated with an incomplete state of knowledge (e.g. Vick, 2002). For example, the hydraulic conductivity (K, units of L/T) of a soil layer takes on a range of values depending on location within the deposit and can be represented by a probability distribution (aleatory uncertainty), whereas the uncertainty associated with the value of K at a specific location, other than at a location where it was measured, is epistemic. Distinguishing between the two types of uncertainty is important for incorporating results of a stochastic analysis into the design of a system component (Der Kiureghian and Ditlevsen, 2009).

In this study, performed as a part of a larger effort to evaluate the influence of vegetation on levee performance (Lanzafame and Sitar, 2018), the authors discuss the application of reliability analysis for stochastic assessment of embankment performance while accounting for the uncertainty in hydraulic properties of the embankment soil. Specifically, the first-order reliability method (FORM) (Zhang and Der Kiureghian, 1995) is used because it is invariant and, therefore, the solution is not dependent on how the mechanistic model is formulated (Hasofer and Lind, 1974). Furthermore, when compared to simplified reliability methods or importance sampling methods (e.g. Monte Carlo), FORM can reach a solution with a relatively small number of model evaluations and provides a number of additional quantitative results for evaluating both aleatory and epistemic uncertainty, including parameter importance and sensitivity measures (Der Kiureghian, 2005; Ditlevsen and Madsen, 2005). Finally, from a practical perspective, levee design and maintenance decisions often must be

prioritised under the restriction of limited resources. The stochastic analyses described herein provide a direct quantitative comparison (i.e. probability) between failure modes considering the range of likely values for key properties. They also identify properties with the greatest impact on the computed results, which is invaluable in guiding investigations and in the overall decision-making process.

Model embankment

Analyses in this study assume a model embankment similar to those found on the Sacramento River in California, USA, specifically, a sandy embankment situated on top of a low hydraulic conductivity layer of silt and/or clay and a high hydraulic conductivity layer of sandy material (Figure 1). The low-hydraulic-conductivity layer represents the native ground surface, a fine-grained fluvial overbank deposit that is generally continuous and relatively thin, extending from the channel into the adjacent floodplain, and commonly referred to as a blanket layer (Batool *et al.*, 2015; Meehan and Benjasupattananan, 2012). A relatively thick sandy aquifer provides a high-hydraulic-conductivity connection to the river and in combination with the blanket layer represents the embankment foundation. The embankment is 5·2 m tall (H_E) with a 6·6 m wide crown and 2·5:1 H:V slopes; a 6·1 m wide berm is located along the waterside toe at the top of the blanket layer (5·5 m average thickness), with the riverbed 10·7 m below the landside toe. During periods of high water, the seepage path of concern for underseepage and slope stability failure modes is from the channel to the landside ground surface through horizontal flow through the aquifer and vertical flow through blanket. The hydraulic gradient is greatest in the blanket layer due to the high contrast in hydraulic conductivity with the underlying aquifer and increases the likelihood of foundation erosion and slope failure. Soil properties and subsurface geometry were selected using existing geotechnical data (GEI Consultants, Inc. and HDR, 2015), and the embankment is marginally stable when the channel water level reaches the embankment crest (i.e. slope stability $F \approx 1{\cdot}0$). The water surface elevation (WSE) corresponding to the 200-year return period flood level is used for deterministic and stochastic analyses herein due to its role as a reference case for the current levee design standards in California (URS, 2014).

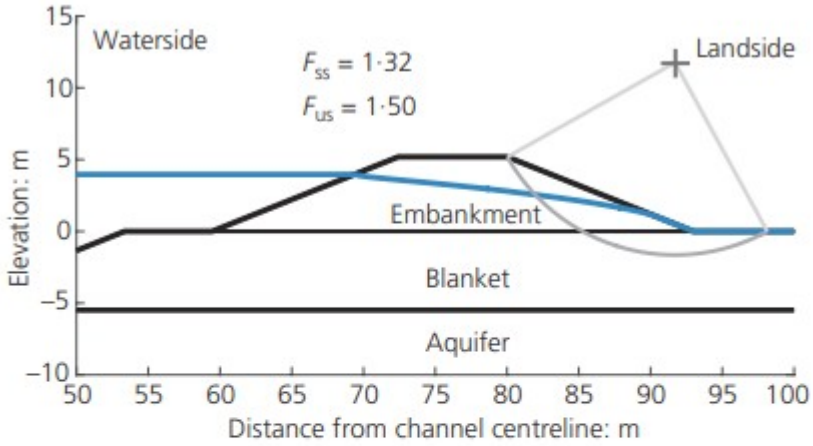

Figure 1. Cross-section of model embankment illustrating phreatic surface for the 200-year return period flood level under steady-state seepage conditions. The factor of safety (F) for heave/uplift is F_{us} = 1·5, and that for the critical (i.e. minimum F_{ss}) sliding surface is F_{ss} = 1·3, using effective stress strength properties. The embankment is 5·2 m tall and underlain by a 5·5 m thick blanket layer (z_B). A blanket layer condition exists, where the vertical hydraulic conductivity of the blanket, $K_{b,v}$, is lower than the horizontal K of the aquifer, $K_{a,h}$. The hydraulic conductivity ratio is evaluated in reliability analyses, where $K_r = K_{a,h}/K_{b,v}$

Analytical Methods

Seepage within the embankment and foundation is governed by the difference in total hydraulic head, h, between the channel and the landside of the embankment, for which a phreatic condition at the ground surface is assumed. The distribution of pore pressure was evaluated using a saturated–unsaturated transient finite-element code, Unsat1 (Neuman, 1972), with transient parameters set to reach steady-state conditions. A finite-element mesh with approximately 9000 rectangular elements was generated with three boundary conditions: constant head on the vertical sides and channel-side ground surface; impermeable boundaries on the aquifer base and embankment crest; and constant-head seepage face conditions on the landside ground surface and embankment slope. Elements range in size from 1·5 m near the boundaries to 0·2 m in and near the embankment, with a maximum aspect ratio of 3:1. As found by Benjasupattananan (2013), the model was relatively insensitive to the presence of an aquitard below the 9·8 m thick aquifer and thus was not included in the finite-element mesh. As such, once steady-state conditions are reached, the computed seepage forces depend only on WSE in the channel and the hydraulic conductivity of the blanket and aquifer, K_b and K_a (for a constant cross-sectional geometry), respectively.

The underseepage failure mode is controlled by internal piping of the foundation, which depends on the initiation and progression of erosion from the landside to waterside beneath the embankment (e.g. Sibley *et al.*, 2017). For the analyses herein, the factor of safety against heave/uplift of the blanket layer is used as a surrogate for assessing internal erosion piping and is evaluated using the effective stress method (e.g. Duncan *et al.*, 2011): the ratio of critical gradient, i_c, to vertical gradient measured across the blanket layer (i) at the landside embankment toe, $F_{us} = i_c/i$. The critical gradient is the ratio of buoyant blanket layer soil unit weight to that of water, $i_c = (\gamma_B - \gamma_w)/\gamma_w$, whereas i is found from the vertical change in head across the blanket divided by blanket layer thickness, $i = h_B/z_B$. Note that a condition of $F_{us} < 1{\cdot}0$ for critical gradient does not imply failure of the entire embankment, but rather it represents a high potential for internal erosion, which may eventually progress to complete failure, in this case a breach, if not addressed.

Slope stability was evaluated using Spencer's method of slices (Spencer, 1967). Drained conditions (steady-state effective stress analysis) and a Mohr–Coulomb failure envelope (i.e. cohesion, c', and friction angle, ϕ') were assumed to estimate soil strength (Shewbridge and Schaefer, 2013). The pore pressures obtained from seepage analyses were applied at the base of each slice. Pore pressures were assumed to be zero above the phreatic line within the embankment – that is, negative pore pressures were assumed to play no role in slope stability. Note that a condition of $F_{ss} < 1{\cdot}0$ for slope stability does not imply failure of the entire embankment, but rather the anticipated failure of an embankment to provide a stable slope, which may eventually lead to complete failure (embankment breach) if not addressed.

Reliability of the embankment is quantified by probability of failure, p, for underseepage and slope stability failure modes

1. $p = P[F(\boldsymbol{x}) \leq 1{\cdot}0]$

where x is a vector of random variables, the mechanical model parameters considered stochastically with a probability distribution function (PDF), as opposed to a deterministic value, and $F(\boldsymbol{x}) \leq 1{\cdot}0$ is the limit state. $P[\cdot]$ represents the unknown cumulative distribution function (CDF) of $F(\boldsymbol{x})$, the conceptual objective of a reliability analysis, which is dependent on the random variable PDFs and the mechanical model used to define the limit state. For practical problems, there is no closed-form solution for the multivariate probability distribution of $F(\boldsymbol{x})$ and various approximate methods are used to solve p. Reliability is evaluated herein with FORM, and the improved Hasofer–Lind/Rackwitz–Flessler (iHL-RF) algorithm (Zhang and Der Kiureghian, 1995) is implemented in Ferum (Bourinet, 2010), Matlab-based reliability software. To provide a numerically robust solution and ensure invariance, all computations are transformed from the original space (i.e. $\boldsymbol{x}$ -space) to the standard normal space (i.e. $\boldsymbol{u}$ -space) using the

Rosenblatt transformation such that $\boldsymbol{u} = T(\boldsymbol{x})$ (Der Kiureghian *et al*., 2006). The iHL-RF algorithm iteratively finds the combination of random variables, $\boldsymbol{u}^*$, such that $F(T^{-1}(\boldsymbol{u}^*)) = 1{\cdot}0$, and the probability density $P[F(T^{-1}(\boldsymbol{u}^*)) = 1{\cdot}0]$ is maximised. Values in $\boldsymbol{u}^*$ are collectively referred to as the design point and when transformed back to the original space as $\boldsymbol{x}^* = T^{-1}(\boldsymbol{u}^*)$ represent the mechanistic model parameter values most likely to exist at the limit state, $F(\boldsymbol{x}) = 1{\cdot}0$. The probability of failure is the integration of probability density beyond the limit state, which is computed in FORM using a linear (i.e. first-order) half-space approximation of the limit-state function at the design point. It follows from linear algebra that the unit normal vector to the half-space approximation, $\boldsymbol{\alpha}$, can be used to find the distance from the $\boldsymbol{u}$-space origin to the design point, $\beta = \boldsymbol{\alpha u}^*$, the reliability index. Probability is computed from β using the multivariate normal CDF, $p = \Phi[-\beta]$. The vector $\boldsymbol{\alpha}$ is the negative normalised limit-state function gradient, containing one element for each random variable

$$\alpha = -\frac{\nabla_x F\left(T\left(\boldsymbol{u}^*\right)\right)}{\left|\nabla_x F\left(T\left(\boldsymbol{u}^*\right)\right)\right|} \quad (2.)$$

An element in α quantifies the contribution of variance of a random variable to the overall variance in F, and the unit vector property (i.e. $\sum_i \alpha_i^2 = 1$) allows for relative comparison with magnitude. For this reason, $\boldsymbol{\alpha}$ is called the importance vector, where the magnitude indicates relative importance for β and the sign indicates whether the random variable functions as a capacity ($\alpha_i < 0$) or demand ($\alpha_i > 0$) on F. Alternative reliability methods, for example, second moment (Ang and Cornell, 1974), Taylor or point estimate (USACE, 1999), only estimate the mean and standard deviation of $F(\boldsymbol{x})$ in the original space to produce β, whereas FORM finds the most likely failure condition and quantifies the contribution of uncertainty through partial derivatives of the solution with respect to each random variable.

Parameter sensitivity can be explicitly quantified using partial derivative computations that are automatically evaluated during a FORM analysis. Whereas the importance vector, $\boldsymbol{\alpha}$, is based on the limit-state function gradient with respect to each random variable, sensitivity vectors can be formulated that quantify the gradient of reliability index with respect to the mean and standard deviation of each random variable, $\nabla_\mu \beta$ and $\nabla_\sigma \beta$ (ref). When scaled by standard deviation of each random variable (σ_x, a row vector) the sensitivity vectors become dimensionless and are referred to as the importance vectors $\boldsymbol{\delta}$ and $\boldsymbol{\eta}$ (Der Kiureghian, 2005)

$$\delta = \nabla_\mu \beta \sigma_x \quad \text{and} \quad \eta = \nabla_\sigma \beta \sigma_x \quad (3.)$$

Sensitivity can be generalised to represent the partial derivative with respect to any distribution parameter in the set θ using the notation $\nabla_\theta \beta$, a row vector with each element consisting of the partial derivative of β with respect to distribution parameter θ_j: $\partial\beta/\partial\theta_j$.

Fragility curves are used to convey the aleatory uncertainty of a particular system as a plot of failure probability against load (Casciati and Faravelli, 1991) – for example, seismic hazard (Gardoni *et al*., 2002a) and flood defences (Simm *et al*., 2008; USACE, 2010). For the embankment considered herein, fragility curves are constructed using β from separate reliability analyses with WSE set to various deterministic values. Following Der Kiureghian (1989) and Gardoni *et al*. (2002b), it is possible to use FORM to estimate the standard deviation of β, σ_β, due to the variance in n parameters, θ, as follows

4. $$\sigma_\beta \approx \sqrt{\left(\frac{\partial\beta}{\partial\theta_1}\sigma_{\theta_1}\right)^2+\left(\frac{\partial\beta}{\partial\theta_2}\sigma_{\theta_2}\right)^2+\cdots+\left(\frac{\partial\beta}{\partial\theta_n}\sigma_{\theta_n}\right)^2}$$

Note that a standard deviation must be assigned to θ_j, which can conceptually be considered a 'distribution of a distribution', and adds an additional layer of complexity to the analysis. However, this allows $\pm\sigma_\beta$ confidence bounds to be placed on the fragility curves, $P[\mu_\beta]$, computed after the equation

5. $$P\left[\beta \pm \sigma_\beta\right] = \left\{\Phi\left(\beta - \sigma_\beta\right), \Phi\left(-\beta + \sigma_\beta\right)\right\}$$

Because σ_β is based on the standard deviation of distribution parameters, it represents a source of epistemic uncertainty for the embankment, as the true value is unknown. Uncertainty associated with distribution parameters is the only source of epistemic uncertainty considered for analyses herein, which represents a relatively small portion of the overall epistemic uncertainty. For example, spatial variability and model uncertainty are two other sources of epistemic uncertainty that are not considered in the analyses presented here.

FORM can also be used to estimate the first and second moments of $F(\boldsymbol{x})$, μ_{FS} and σ_{FS}, using the definition of reliability index, $\beta = \sigma/\mu$, and the first-order approximation of the limit state at the design point

6. $$\sigma_{FS} = |\nabla F(\boldsymbol{x}^*)|$$

Thus, the stochastic F confidence bounds on a mean estimate of F can be constructed (i.e. $\mu_{FS} \pm \sigma_{FS}$), which represent the effect of aleatory uncertainty in the random variables on F. Furthermore, the mean estimate of F can be compared to the deterministic analysis, which employs the 'best-

estimate' values rather than the entire probability distribution for each random value.

Random variables and probability distributions

The variables that directly influence the underseepage failure mode are the hydraulic conductivity ratio (K_r), the blanket layer thickness (z_B) and the unit weight (γ_B). These three variables indirectly influence slope stability by controlling seepage forces, while the variables that directly influence the slope failure mode are the embankment unit weight (γ_E) and friction angle (ϕ'_E), blanket unit weight (γ_B), effective cohesion (c'_B) and friction angle (ϕ'_B). Note that γ_B has a direct influence on both failure modes. The variability of these random variables is summarised in Table 1 using the coefficient of variation, $\delta = \sigma/\mu$, along with the values used for reliability analyses described herein. These parameters were obtained from published sources, as noted in the table, and from subsurface data collected during investigations at the site of the prototype embankment (GEI Consultants, Inc. and HDR, 2015).

Table 1. Soil properties analysed as random variables and associated probability distributions

RV	Unit	Type	δ (typical)[a]	Distribution	μ	σ	δ
γ_B	kN/m^3	Seepage/stability	0·05–0·10	N(μ,σ)	18·1	1·81	0·05
c'_B	kPa	Stability	0·10–0·30	N(μ,σ)	1·20	0·36	0·30
ϕ'_B	°	Stability	0·05	N(μ,σ)	36·0	1·80	0·05
γ_E	kN/m^3	Stability	0·05–0·10	N(μ,σ)	18·9	1·32	0·07
ϕ'_E	°	Stability	0·05	N(μ,σ)	38·0	1·90	0·05
K_r	—	Seepage	0·30–3·00	LN(λ,ζ)[b]	1600[c]	39 200	4·90
z_B	m	Seepage	—	tN(μ,σ,z_1,z_2)[d]	5·54	1·71	0·31

[a] Typical values, summarised from Baecher and Christian (2003), Uzielli *et al.* (2006) and USACE (1999)
[b] $K_r \approx$ LN(7·38,1·79); $K_{b,v}$ is found for a given K_r with $K_{a,h} = 8 \times 10^5$ m/s; $\delta = 2·0$ for $K_{b,v}$ and $K_{a,h}$
[c] The median value is 1600, which is used in deterministic analyses; the arithmetic mean is 8000
[d] $z_B \approx$ tN(5·49,1·87,1·70,10·0)
LN, lognormal; N, normal; RV, random variable; tN, truncated normal
Mean values of distribution, μ, were used in deterministic analyses, except as noted for non-normal distributions

The random variables controlling slope stability were modelled using the normal distribution, with parameters μ and σ derived from field data that matched well with typical values of δ from the literature. The lognormal distribution was used to describe the variability of K because it often ranges over several orders of magnitude and is non-negative (Freeze, 1975). Reported δ varies widely for K (Benson, 1993), although 0·3–2·0 is commonly cited (e.g. USACE, 1999; Uzielli *et al.*, 2006). Published data sets with test results that support reported values of δ for K are relatively limited (Lanzafame, 2017; Lanzafame and Sitar, 2018), and it is unclear whether the high variability is due to aleatory or epistemic uncertainty. While a probability distribution and associated δ imply aleatory variability, errors from field and laboratory tests as well as inclusion of data collected over a relatively large regional extent imply that epistemic uncertainty may have a significant role in reported δ. For analyses herein, deterministic values of the horizontal hydraulic conductivity of the aquifer, $K_{a,h}$, and the vertical hydraulic conductivity of the blanket layer, $K_{b,v}$, were used to fix the mean

values of the lognormal distributions and δ is set to a conservative value of 2·0, near the upper end of values found for a suite of alluvial near-surface soils in California (URS, 2014). Lognormal distribution parameters λ and ζ are the mean and standard deviation of $\ln K$.

The ratio of hydraulic conductivity is more important than absolute values for controlling the distribution and magnitude of seepage forces (Batool *et al.*, 2015; Chowdhury *et al.*, 2012; USACE, 1999), and incorporating $K_{a,h}$ and $K_{b,v}$ as a single random variable reduces the necessary number of computations in a reliability analysis. Hydraulic conductivity ratio is defined as $K_r = K_{a,h}/K_{b,v}$; thus, for a particular value of K_r infinite combinations of $K_{a,h}$ and $K_{b,v}$ are available and only one set must be selected as parameters to specify in the finite-element method (FEM) seepage model. However, the seepage solution is insensitive for K_r less than about 50 for the model levee considered herein (Lanzafame *et al.*, 2017), and for a given K_r, the value of $K_{b,v}$ is chosen such that $K_{a,h} = 8 \times 10^{-5}$ m/s. K is anisotropic ($K_h = 4K_v$) for the blanket layer and isotropic for the embankment and aquifer soils. Lognormal distribution parameters for K_r can be determined as a function of the random variables $K_{a,h}$ and $K_{b,v}$ as follows (Table 1)

$$7. \quad \lambda_r = \lambda_a - \lambda_b \quad \text{and} \quad \zeta_r = \sqrt{\zeta_a^2 + \zeta_b^2}$$

where the subscripts r, a and b refer to K_r, aquifer and blanket, respectively. The skewness of the distribution results in a mean value of 8000 and a median ($\ln \lambda_r$) of 1600 for K_r.

The blanket layer thickness, z_B, was modelled with a truncated normal distribution, which adds maximum and minimum values as parameters and redistributes the normal probability density function within these limits (e.g. Kottegoda and Rosso, 2008). Although modifications to the PDF with respect to the normal distribution are not negligible, the lower limit (z_1) is occasionally necessary to prevent errors in the FEM seepage analysis (Lanzafame and Sitar, 2018). The truncated normal distribution does not significantly affect reliability results as long as the design point from a FORM solution is not close to the distribution limits (Lanzafame and Sitar, 2018).

Results

Deterministic analyses of underseepage and slope stability were completed for various hydraulic loads. At the 200-year WSE, the phreatic surface exits the landside embankment slope at the breakout height, 2·1 m above the landside toe elevation (Figure 1), and the deterministic factors of safety for underseepage and slope stability failure are $F_{us} = 1{\cdot}5$ and $F_{ss} = 1{\cdot}3$, respectively. The change in the deterministic factors of safety with increasing water level for the two failure modes is presented in Figure 2. The results show that the factor of safety for slope stability decreases to 1·0 and

the factor of safety for underseepage decreases to 1·2 as the water level reaches the crest of the embankment.

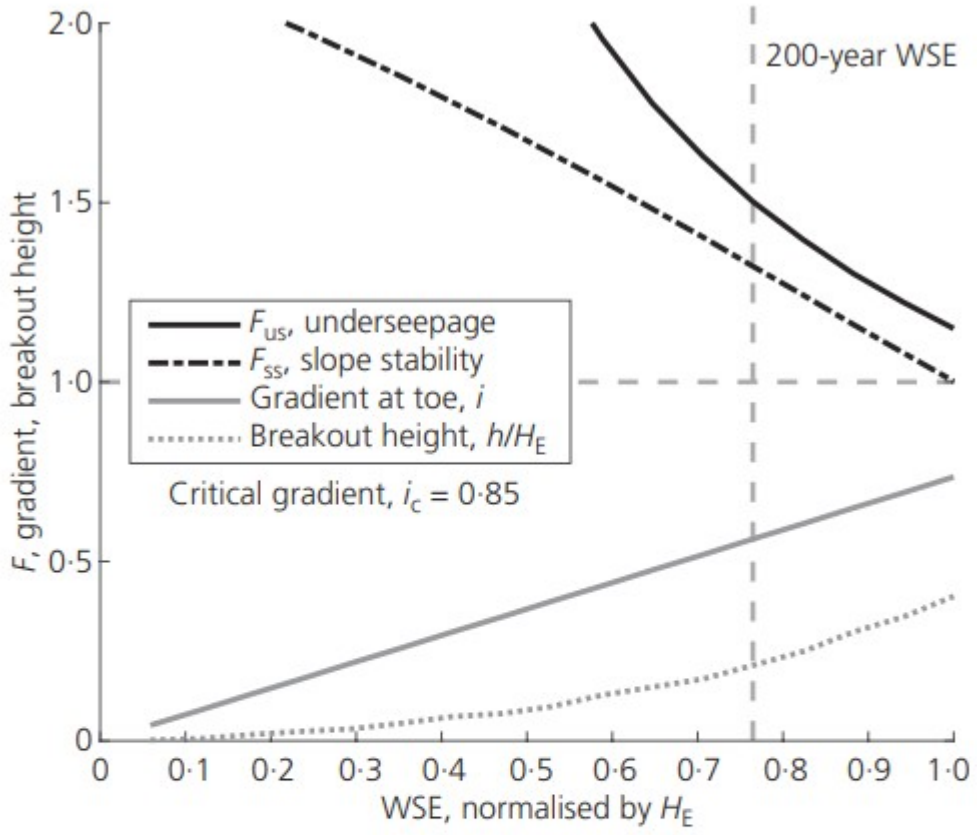

Figure 2. Deterministic results for factor of safety (F) for embankment underseepage and slope stability across all water levels (WSE), normalised by embankment height. Underseepage is assessed using F for heave/uplift, limit equilibrium slope stability, steady-state seepage conditions and effective stress strength parameters (Mohr–Coulomb). Gradient is measured vertically across the blanket layer at the landside embankment toe. The breakout height is the elevation above the toe where the phreatic surface exits the landside slope, normalised by the embankment height (h/H_E)

Reliability results from the FORM analyses are summarised in Tables 2 and 3 and consist of the probability of exceeding the set limit state, p, the value of the parameter at the point with the highest probability of failure, x^*, and the importance vectors $\boldsymbol{\alpha}$, $\boldsymbol{\delta}$ and $\boldsymbol{\eta}$. The probability of an unsafe condition, $P[F \leq 1{\cdot}0]$, is 0·17 for underseepage ($\beta = 0{\cdot}98$) and 0·06 for slope stability ($\beta = 1{\cdot}54$). While the likelihood of failure is an important measure of risk, from a practical perspective, the importance vectors have a much greater significance since they show which parameter(s) has the greatest effect on

the computed result. Thus, for underseepage (Table 2) the importance vector, $\boldsymbol{\alpha}$, for blanket layer thickness (z_B) has the largest magnitude, showing that the blanket layer thickness is the most important random variable, followed by the blanket unit weight (γ_B), with the hydraulic conductivity ratio (K_r) an order of magnitude less. In this case, the variables z_B and γ_B are capacity variables (i.e. $\alpha_i < 0$), whereas K_r is a demand variable, which is consistent with the design point (x^* and u^*), indicating that the critical condition for underseepage is when z_B and γ_B have values less than the median and K_r has a value above the median. Because z_B is the most important random variable, the design point has the highest deviation from the median, $u_i^* = -0 \cdot 9$. Importance vectors for the distribution mean and standard deviation (δ and η) confirm the general importance of z_B while also showing that the value of the mean has a bigger effect on reliability than the standard deviation for K_r and γ_B, as $\delta_i > \eta_i$ for both variables. Again, from a practical standpoint, this result suggests that measuring the thickness of the blanket layer is more important than measuring its hydraulic conductivity. Since obtaining the thickness of the blanket at multiple locations is much simpler than measuring its hydraulic conductivity, this is very useful information that would not have been as apparent from other types of analyses.

Table 2. FORM results for underseepage failure mode, evaluated at the 200-year water level, including design point (original, x^*, and standard normal space, u^*), importance vectors ($\boldsymbol{\alpha}$), statistically scaled sensitivity of mean (δ) and standard deviation (η)

RV	x^*	u^*	α	δ	η
K_r	1900	+0·095	+0·098	−0·509	+0·050
z_B	3·89 m	−0·914	−0·936	−1·970	+1·790
γ_B	17·6 kN/m^3	−0·329	−0·337	+0·337	−0·111

$\beta = 0{\cdot}976$ and $p = 0{\cdot}165$

Table 3. FORM results for slope stability failure mode, evaluated at the 200-year water level, including design point (original, x^*, and standard normal space, u^*), importance vectors ($\boldsymbol{\alpha}$), statistically scaled sensitivity of mean ($\boldsymbol{\delta}$) and standard deviation ($\boldsymbol{\eta}$)

RV	x^*	u^*	α	δ	η
K_r	2170	+0·170	+0·110	−0·563	+0·054
z_B	3·07 m	−1·410	−0·921	−2·780	+1·480
γ_B	17·5 kN/m^3	−0·482	−0·313	+0·313	−0·151
c'_B	1·13 kPa	−0·179	−0·116	+0·116	−0·021
ϕ'_B	35·7°	−0·145	−0·094	+0·094	−0·014
γ_E	18·6 kN/m^3	−0·180	−0·117	+0·117	−0·021
ϕ'_E	37·8°	−0·124	−0·081	−0·081	−0·010

$\beta = 1{\cdot}537$ and $p = 0{\cdot}062$

Similarly, for the slope stability failure mode, z_B and γ_B are also the most important random variables (Table 3). The importance of K_r is of similar magnitude to c'_B and γ_E, with ϕ'_E and ϕ'_B being the least important variables. As with underseepage, K_r is the only demand variable and the design point indicates that the critical condition is a thin blanket layer. This result has a clear physical meaning, since the blanket layer acts to resist the base failure and, therefore, its thickness and weight will have a significant influence on the computed factor of safety. The results also show that the value of cohesion used in the analyses has a greater influence than the value of the friction angle, hence focusing the attention on that particular parameter in embankment design.

Fragility curves for underseepage and slope stability are presented in Figures 3 and 4 for water levels between the embankment toe and crest elevations. Each point on the fragility curve represents the probability of exceeding the limit state for a specific WSE due to the probability distribution specified for each random variable. Thus, the value of p (and β) at each WSE is a result of the aleatory uncertainty contribution from each random variable, which is quantified in Figures 3 and 4 with the importance vector, $\boldsymbol{\alpha}$. Values of $\boldsymbol{\alpha}$ in Figures 3 and 4 are from FORM results for the 200-year WSE, which remained consistent across the range of WSEs considered. Because the estimate of β is dependent on the parameters used for each random variable probability distribution, there is uncertainty in the calculated value at each WSE, which is quantified using the confidence interval σ_β (Equation 4). Thus, the confidence bounds for fragility (Equation 5) in Figures 3 and 4 quantify a subset of the epistemic uncertainty for each failure mode, and the individual contribution from each random variable is also ranked and tabulated. For underseepage and slope stability, z_B is the greatest source of epistemic

uncertainty, although γ_B has comparable level of influence for the underseepage failure mode.

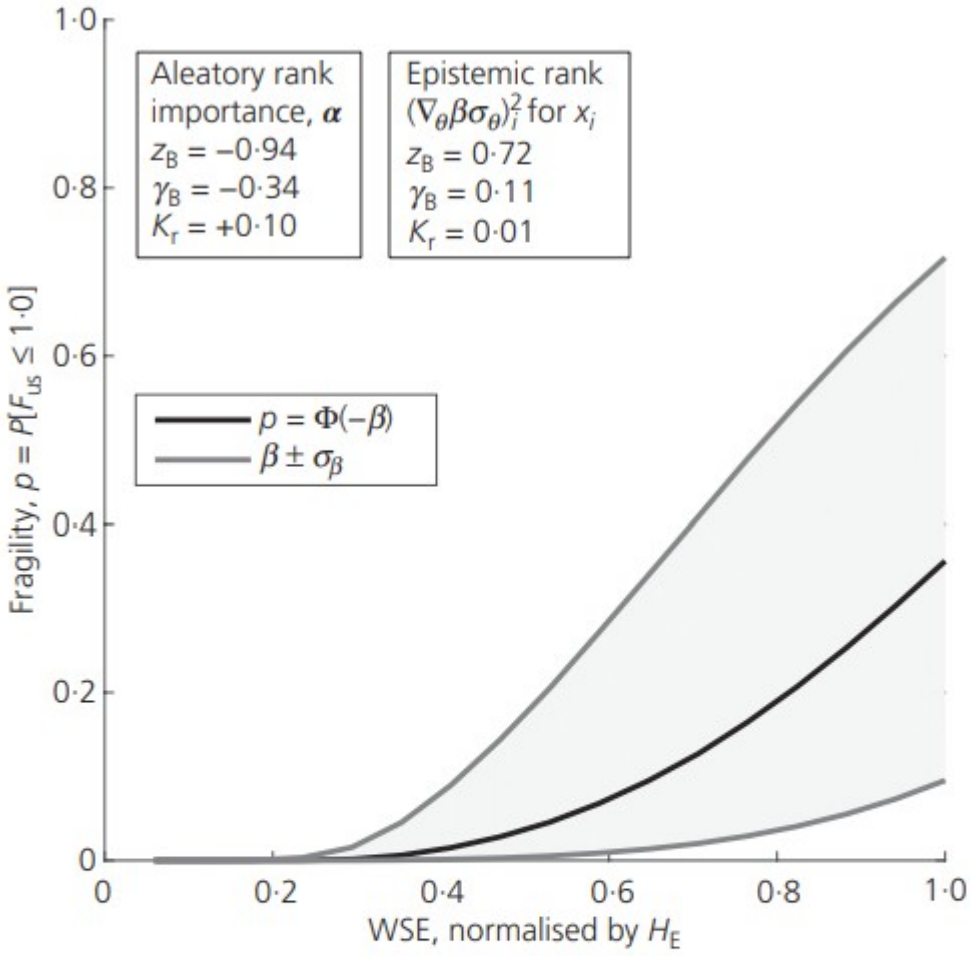

Figure 3. Fragility curve for underseepage illustrates aleatory variability at various flood levels, normalised by embankment height. Fragility is computed with FORM as $p = P[F_{us} \leq 1{\cdot}0]$, where F_{us} is the factor of safety against heave/uplift. The contribution of each random variable to aleatory and epistemic uncertainty is ranked by magnitude. Confidence interval for fragility, σ_β, is computed from uncertainty in probability distribution parameters, which represents a subset of overall epistemic uncertainty in fragility

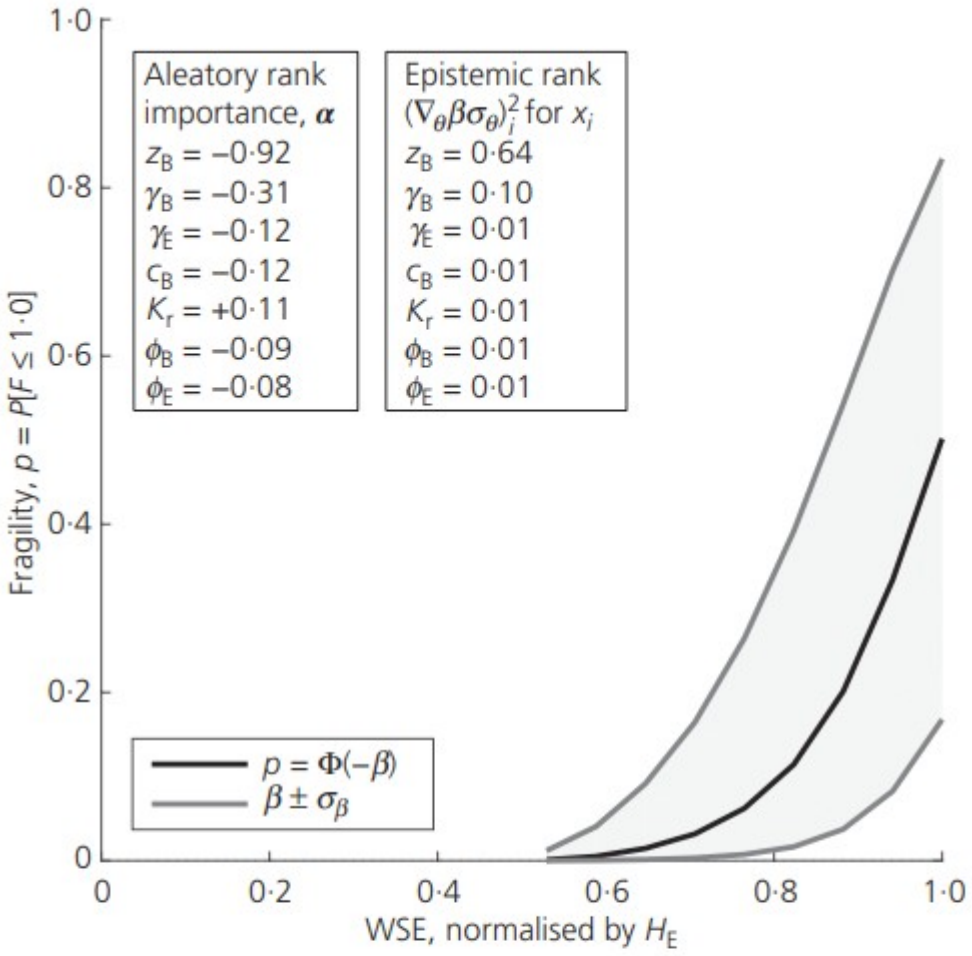

Figure 4. Fragility curve for slope stability illustrating aleatory variability at various flood levels, normalised by embankment height. Fragility is computed with FORM as $p = P[F_{ss} \leq 1·0]$, where F_{ss} is the factor of safety of the minimum F sliding surface. The contribution of each random variable to aleatory and epistemic uncertainty is ranked by magnitude. Confidence interval for fragility, σ_β, is computed from uncertainty in probability distribution parameters, which represents a subset of overall epistemic uncertainty in fragility. Slope stability reliability is not computed for WSE below $0·5H_E$ due to numerical problems with Spencer's method of slices

The stochastic estimate of F using FORM (μ_{FS}) is illustrated in Figures 5 and 6 for various WSEs, along with the confidence interval given by $\mu_{FS} \pm \sigma_{FS}$. This represents the expected value of F (at each WSE), given the range of values possible (i.e. aleatory variability) for each parameter assigned a probability distribution. The individual contribution of each random variable is tabulated and ranked on the figures using the importance vector, $\boldsymbol{\alpha}$. As WSE increases

and approaches the embankment crest elevation, μ_{FS}, for underseepage and slope stability decreases to 1·2 and 1·0, with the confidence intervals ±0·4 and ±0·2, respectively. Figures 5 and 6 also compare deterministic F (Figure 2) to μ_{FS}, which is a comparison of F computed using the mean values of each parameter against the mean value of F given the aleatory variability in each parameter (i.e. the complete probability distribution, as opposed to only the mean), respectively. Given that μ_{FS} is from FORM and has an invariant solution, it is a better estimate of the expected value for F. For the deterministic case where $F = 1{\cdot}0$, the design point is nearly equivalent to the mean values of each random variable; thus, F and μ_{FS} are equivalent. At the 200-year WSE, the deterministic F is 0·04 greater than the median value of the factor of safety, μ_{FS}, for underseepage (unconservative F), but 0·20 below μ_{FS} for slope stability (conservative F). Although the deterministic and stochastic assessments of F are not identical, differences are less than the confidence interval for μ_{FS}, which is governed by aleatory uncertainty in the input random variables. As illustrated by the ranked values on Figures 5 and 6, reducing uncertainty in z_B and γ_B will result in the greatest reduction of uncertainty for underseepage and slope stability F.

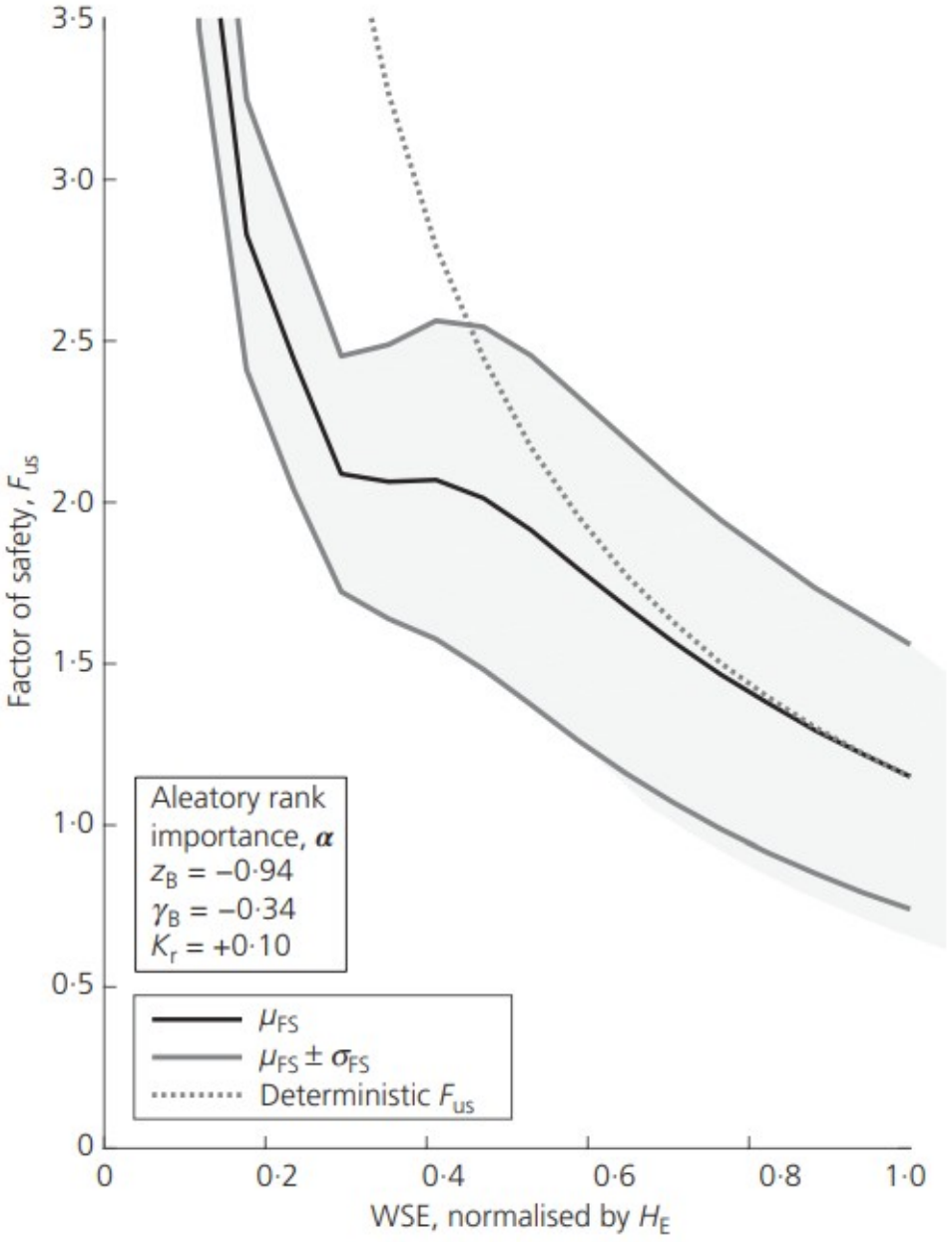

Figure 5. Stochastic F curve (μ_{FS}) for underseepage illustrates expected value of F_{us} at various flood levels, normalised by embankment height. The contribution of each random variable to aleatory uncertainty is ranked by magnitude. The confidence interval for μ_{FS} is found from $\pm\sigma_{FS}$ and is related to the aleatory variability of random variables (α). Deterministic F_{us} is compared to stochastic case and is within $\mu_{FS} \pm \sigma_{FS}$. The irregular shape of the μ_{FS} curve is due to the design point for z_B approaching the lower truncated normal distribution limit (z_1) as β increases with decreasing WSE

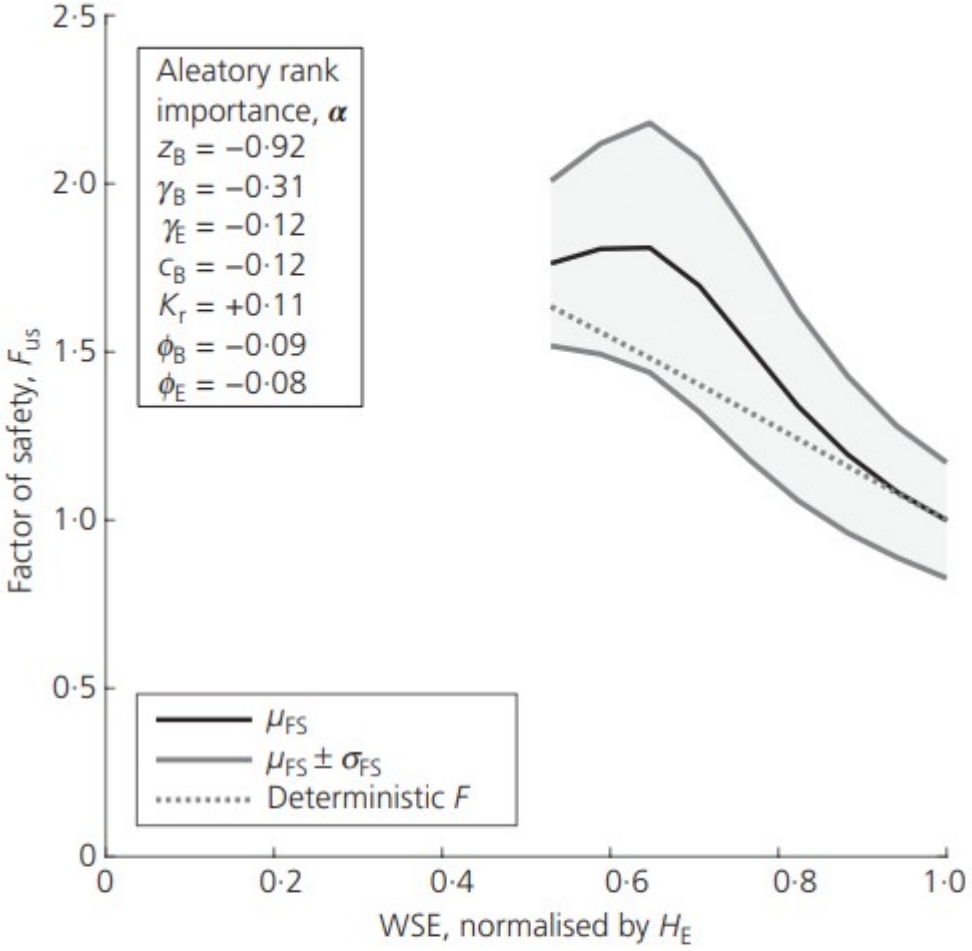

Figure 6. Stochastic F curve (μ_{FS}) for slope stability illustrates expected value of F_{ss} at various flood levels, normalised by embankment height. The contribution of each random variable to aleatory uncertainty is ranked by magnitude. The confidence interval for μ_{FS} is found from $\pm\sigma_{FS}$ and is related to the aleatory variability of random variables (α). Deterministic F_{ss} is compared to stochastic case and is within $\mu_{FS} \pm \sigma_{FS}$. The irregular shape of the μ_{FS} curve is due to the design point for z_B approaching the lower truncated normal distribution limit (z_1) as β increases with decreasing WSE. Slope stability reliability is not computed for WSE below $0{\cdot}5H_E$ due to numerical problems with Spencer's method of slices

To illustrate further the role of stochastic seepage properties on embankment performance, probability distribution parameters were varied for K_r and z_B. The lognormal distribution of K_r was evaluated with a median value ($\exp\lambda$) of 1000, 100 and 10, each with a δ of 0·3 and 2·0 for K (cases A–F). The truncated normal distribution of z_B was modified by reducing δ and

modifying the upper and lower truncation limits, z_1 and z_u (cases G–J). Changes in β and p are tabulated in Table 4 for the ten cases considered, in addition to changes in importance, α_i, for K_r, z_B and γ_B. As expected, reducing δ increases β and decreases p for both failure modes. Reducing the median of K_r increases β and the importance of K_r while decreasing the importance of z_B, although Imp(z_B) > Imp(K_r) for cases A–F. Removing the upper truncation limit for z_B has a negligible effect (case G), whereas increasing the lower truncation limit (cases H and I) changes β and α by a small amount.

Table 4. Probability distribution effects for z_B and K_r: comparison of FORM results for alternate distribution parameters for K_r and z_B, evaluated at the 200-year water level

Variation from reference case (Table 1)			Underseepage					Slope stability				
			β	p	Importance, α_i			β	p	Importance, α_i		
					K_r	z_B	γ_B			K_r	z_B	γ_B
Reference case			0·97	0·165	+0·10	−0·94	−0·34	1·54	0·062	+0·11	−0·92	−0·31
A	K_r	exp(λ) = 1000, δ = 0·3	1·02	0·154	+0·04	−0·94	−0·34	1·60	0·055	+0·05	−0·92	−0·32
B	K_r	exp(λ) = 1000, δ = 2·0	1·00	0·158	+0·14	−0·93	−0·34	1·57	0·058	+0·15	−0·91	−0·31
C	K_r	exp(λ) = 100, δ = 0·3	1·56	0·059	+0·16	−0·92	−0·34	2·31	0·010	+0·24	−0·84	−0·40
D	K_r	exp(λ) = 100, δ = 2·0	1·36	0·087	+0·42	−0·85	−0·31	1·92	0·027	+0·42	−0·83	−0·30
E	K_r	exp(λ) = 10, δ = 0·3	2·82	0·002	+0·30	−0·78	−0·54	4·23	1×10^{-5}	+0·40	−0·52	−0·62
F	K_r	exp(λ) = 10, δ = 2·0	2·04	0·021	+0·61	−0·75	−0·28	2·61	0·005	+0·63	−0·69	−0·29
G	z_B	δ = 0·32, $x_u = \infty$	0·96	0·168	+0·10	−0·94	−0·33	1·52	0·065	+0·11	−0·92	−0·31
H	z_B	δ = 0·25, x_l = 1·7 m	1·20	0·114	+0·11	−0·89	−0·44	1·88	0·030	+0·12	−0·87	−0·40
I	z_B	δ = 0·23, x_l = 3·0 m	1·16	0·122	+0·13	−0·85	−0·51	1·98	0·024	+0·13	−0·71	−0·58
J	z_B	δ = 0·10, x_l = 3·0 m	1·95	0·025	+0·13	−0·45	−0·88	2·66	0·004	+0·11	−0·27	−0·79

exp(λ) is the median of K_r; λ is a lognormal distribution parameter

Discussion

Despite the high aleatory variability for K and K_r, the blanket layer thickness controls embankment underseepage and slope stability for the high-permeability-contrast blanket layer foundation considered herein. As illustrated in Table 4, the importance of K_r increases as the median value used in stochastic analyses decreases, becoming comparable to that of z_B only when the median of K_r is 10 (cases E and F). Although the trend continues as the median of K_r approaches 1, this implies that the blanket and aquifer are a single homogeneous soil unit since hydraulic conductivity values for the blanket and aquifer becomes equal – that is, the blanket layer foundation condition is no longer applicable. Thus, for a blanket layer condition, the aleatory variability of K_r is more comparable to typical soil shear strength properties, but contributes less to the aleatory variability in F than z_B.

Fragility curves quantify the aleatory variability for each failure mode, as well as a subset of the overall epistemic uncertainty associated with the selection of probability distribution parameters for each random variable. Although the fragility for underseepage is higher than that with respect to slope stability, the computed probability is only for the limit state, $F \leq 1{\cdot}0$, which does not necessarily imply the embankment is more likely to be breached from internal erosion piping against a slope stability failure.

Stochastic F and the confidence interval, $\mu_{FS} \pm \sigma_{FS}$, illustrate the influence of aleatory variability in shear strength and hydraulic properties on the deterministic assessment of F. Given the distribution parameters considered herein, it is clear that underseepage and slope stability failure modes are not necessarily safe if deterministic $F > 1{\cdot}0$, particularly for WSE above the 200-year level. Figures 5 and 6 indicate that the deterministic F is unconservative with respect to the stochastic F for underseepage, but conservative for slope stability, which is a result of the mechanical sensitivity for each failure mode in combination with the aleatory variability for each random variable. The non-linear shape for each stochastic F curve is due to the non-linear relationship of β with increasing WSE as the design point for z_B approaches the lower truncated normal distribution limit z_1.

As the blanket layer thickness is reduced, it cannot be allowed to cross the lower surface of the potential sliding mass for slope stability computations: a constant finite-element mesh is necessary to prevent numerical errors from negatively impacting the solution. Thus, while there is a physical justification for limiting blanket layer thickness with the truncated normal distribution, it can influence FORM results, particularly as the design point for z_B decreases. In general, analyses should be repeated with various z_1 values to confirm that reliability results are not affected. Further, numerical considerations associated with various distribution effects are described by Lanzafame and Sitar (2018).

Analyses discussed herein assume homogeneous seepage and strength properties within each soil unit, which ignores the variation that occurs spatially. The influence of spatial correlation has been previously included in FORM analysis of seepage (Sitar *et al*., 1987) and slope stability problems (Kim and Sitar, 2013), as well as random sampling (e.g. Liu *et al*., 2017). Since the focus of this study was on the relative importance of seepage and strength properties with respect to underseepage and slope stability failure modes, spatial variability would have had relatively minor influence.

Conclusions

Reliability analyses using FORM show that the blanket unit weight and thickness dominate underseepage and slope stability assessments, as expected from deterministic analyses. Hydraulic conductivity does not influence underseepage and slope stability significantly more than typical shear strength parameters, despite the potentially large order of magnitude range in variability, for a blanket layer condition with high contrast with respect to the aquifer. Fragility curves illustrate the influence of aleatory and a subset of epistemic uncertainty, most of which is due to blanket layer thickness and unit weight. In addition to reliability index, stochastic F curves provide a graphical interpretation of the uncertainty in deterministic estimates of F. Reliability analyses provide a useful tool for conveying the risk associated with embankment performance, in this case underseepage and slope stability. Once implemented in software for the particular problem

of interest, FORM analyses are numerically efficient, relative to alternative methods such as Monte Carlo simulation. Using fragility curves and uncertainty estimates provides a straightforward method of comparing aleatory and epistemic uncertainty and directly assessing the relative importance of critical properties. From a practical standpoint, probabilistic analyses allow for a direct quantitative comparison between failure modes and identify the parameters that have the most significant influence on the computed results.

Acknowledgments

This research was performed as part of a California Levee Vegetation Research Program project, funded by California Department of Water Resources Contract Number 4600010737.

References

Ang AH and Cornell CA (1974) Reliability bases of structural safety and design. Journal of the Structural Division 100(ST9): 1077–1769.

ASCE (American Society of Civil Engineers) (2010) So, You Live Behind a Levee!: What You Should Know to Protect Your Home and Loved Ones from Floods. Princeton Architectural Press, Hudson, NY, USA.

Baecher GB and Christian JT (2003) Reliability and Statistics in Geotechnical Engineering. Wiley, Hoboken, NJ, USA.

Batool A, VandenBerge D and Brandon T (2015) Practical application of blanket theory and the finite-element method to levee underseepage analysis. Journal of Geotechnical and Geoenvironmental Engineering 141(4): 1–10, https://doi.org/10.1061/(ASCE)GT.1943-5606.0001269.

Benjasupattananan S (2013) Deterministic and Probabilistic Approaches for Modeling Levee Underseepage. DEng thesis, University of Delaware, Newark, DE, USA.

Benson CH (1993) Probability distributions for hydraulic conductivity of compacted soil liners. Journal of Geotechnical Engineering 119(3): 471–486.

Bourinet J (2010) FERUM 4.1 User’s Guide. Sigma Clermont, Aubière, France. See https://www.sigma-clermont.fr/en/ferum-documentation (accessed 25/05/2016).

Casciati F and Faravelli L (1991) Fragility Analysis of Complex Structural Systems. Research Studies Press, Somerset, UK.

Cedergren HR (1997) Seepage, Drainage, and Flow Nets. Wiley, New York, NY, USA.

Chowdhury K, Millet R, Punyamurthula S, Hong GT and Tollefson N (2012) It is seepage indeed – a sensitivity study on seepage and seepage-induced slope stability of levees. Proceedings of the USSD Annual Meeting and Conference, New Orleans, LA, USA, pp. 659–689.

Der Kiureghian A (1989) Measures of structural safety under imperfect states of knowledge. Journal of Structural Engineering 115(5): 1119–1140, https://doi.org/ 10.1061/(ASCE)0733-9445(1989)115:5(1119).

Der Kiureghian A (2005) First-and second-order reliability methods. In Engineering Design Reliability handbook (Nikolaidis E, Ghiocel DM and Singhal S (eds)). CRC Press, Boca Raton, FL, USA.

Der Kiureghian A and Ditlevsen O (2009) Aleatory or epistemic? Does it matter? Structural Safety 31(2): 105–112, https://doi.org/ 10.1016/j.strusafe.2008.06.020.

Der Kiureghian A, Haukaas T and Fujimura K (2006) Structural reliability software at the University of California, Berkeley. Structural Safety 28(1): 44–67, https://doi.org/ 10.1016/j.strusafe.2005.03.002.

Ditlevsen O and Madsen HO (2005) Structural Reliability Methods. Technical University of Denmark, Kongens Lyngby, Denmark.

Duncan JM and Wright SG (2005) Soil Strength and Slope Stability. Wiley, Hoboken, NJ, USA.

Duncan JM, O'Neil B, Brandon TL and VandenBerge DR (2011) Evaluation of Potential for Erosion in Levees and Levee Foundations. Center for Geotechnical Practice and Research, Virginia Polytechnic Institute and State University, Blacksburg, VA, USA, CGPR-64.

DWR (Department of Water Resources) (2012) Urban Levee Design Criteria. FloodSafe California, Department of Water Resources, Sacramento, CA, USA.

Freeze RA (1975) A stochastic-conceptual analysis of one-dimensional groundwater flow in non-uniform homogeneous media. Water Resources Research 11(5): 725–741, https://doi.org/ 10.1029/ WR011i005p00725.

Gardoni P, Der Kiureghian A and Mosalam KM (2002a) Probabilistic Models and Fragility Estimates for Bridge Components and Systems. Pacific Earthquake Engineering Research Center, University of California–Berkeley, Berkeley, CA, USA, PEER 2002/13.

Gardoni P, Der Kiureghian A and Mosalam KM (2002b) Probabilistic capacity models and fragility estimates for reinforced concrete columns based on experimental observations. Journal of Engineering Mechanics 128(10): 1024–1038, https://doi.org/ 10.1061/(ASCE)0733- 9399(2002)128:10(1024).

GEI Consultants, Inc. and HDR (2015) Embankment and Foundation Stability Memorandum. Sacramento River East Levee Improvement Project, Sacramento, CA, USA.

Harr ME (2012) Groundwater and Seepage. Dover Publications, Mineola, NY, USA.

Hasofer AM and Lind NC (1974) Exact and invariant second-moment code format. Journal of the Engineering Mechanics Division 100(1): 111–121.

Holtz RD and Kovacs WD (1981) An Introduction to Geotechnical Engineering. Prentice Hall, Englewood Cliffs, NJ, USA.

Kelley R (1998) Battling the Inland Sea: Floods, Public Policy, and the Sacramento Valley. University of California Press, Berkeley, CA, USA.

Kim JM and Sitar N (2013) Reliability approach to slope stability analysis with spatially correlated soil properties. Soils and Foundations 53(1): 1–10, https://doi.org/ 10.1016/j.sandf.2012.12.001.

Kottegoda NT and Rosso R (2008) Applied Statistics for Civil and Environmental Engineers. Blackwell, Malden, MA, USA.

Lanzafame R (2017) Reliability Analysis of the Influence of Vegetation on Levee Performance. PhD thesis, Department of Civil and Environmental Engineering, University of California–Berkeley, Berkeley, CA, USA.

Lanzafame R and Sitar N (2018) Reliability Analysis of the Influence of Woody Vegetation on Levee Performance. California Levee Vegetation Research Program, Department of Water Resources, Sacramento, CA, USA, University of California–Berkeley, Berkeley, CA, USA, UCBGT/18/01.

Lanzafame R, Teng H and Sitar N (2017) Stochastic analysis of levee stability subject to variable seepage conditions. In Geo-risk 2017: Reliability-based Design and Code Developments (Huang J, Fenton GA, Zhang L and Griffiths DV (eds)). ASCE, Denver, CO, USA, pp. 554–563.

Liu K, Vardon PJ and Hicks MA (2017) Probabilistic analysis of seepage for internal stability of earth embankments. Environmental Geotechnics, https://doi.org/10.1680/jenge.17.00040.

Meehan CL and Benjasupattananan S (2012) An analytical approach for levee underseepage analysis. Journal of Hydrology 470–471(1): 201–211, https://doi.org/10.1016/j.jhydrol.2012.08.050.

Neuman SP (1972) Finite Element Computer Programs for Flow in Saturated–Unsaturated Porous Media. Hydraulic Engineering Laboratory, Technion–Israel Institute of Technology, Haifa, Israel.

Phoon KK, Becker D, Kulhawy FH et al. (2003) Why consider reliability analysis for geotechnical limit state design? In Proceedings of the International Workshop on Limit State Design in Geotechnical Engineering Practice (Phoon KK, Honjo Y and Golber RB (eds)). World Scientific, Singapore.

Seed RB, Cobos-Roa D, Pestana JM, Athanasopoulos-Zekkos A and Inamine M (2012) U.S. levee and flood protection engineering in the wake of Hurricane Katrina. In Geotechnical Engineering State of the Art and Practice: Keynote Lectures from GeoCongress 2012 (Rollinss K and Zekkos D (eds)). ASCE, Oakland, CA, USA, pp. 294–334.

Shewbridge SE and Schaefer J (2013) Some unexpected ‘modern’ complications in seepage and slope stability analysis: modeling pore

pressures and strengths for flood-loaded structures. Proceedings of 2013 Annual Dam Safety Conference, ASDSO, Providence, RI, USA, pp. 694–714.

Sibley HM, Vroman ND and Shewbridge SE (2017) Quantitative riskinformed design of levees. In Geo-risk 2017: Reliability-based Design and Code Developments (Huang J, Fenton GA, Zhang L and Griffiths DV (eds)). ASCE, Denver, CO, USA, pp. 76–90.

Simm J, Gouldby B, Sayers P et al. (2008) Representing fragility of flood and coastal defences: Getting into the detail. Proceedings of Floodrisk 2008, Oxford, UK, pp. 621–631.

Sitar N, Cawlfield JD and Der Kiureghian A (1987) First-order reliability approach to stochastic analysis of subsurface flow and contaminant transport. Water Resources Research 23(5): 794–804, https://doi.org/10.1029/WR023i005p00794.

Spencer E (1967) A method of analysis of the stability of embankments assuming parallel inter-slice forces. Géotechnique 17(1): 11–26.

URS (2014) Guidance Document for Geotechnical Analyses, v14. California Department of Water Resources, Sacramento, CA, USA.

USACE (US Army Corps of Engineers) (1999) Risk-based Analysis in Geotechnical Engineering for Support of Planning Studies. USACE, Washington, DC, USA, ETL-1110-2-556.

USACE (2000) Design and Construction of Levees. USACE, Washington, DC, USA, EM 1110-2-1913.

USACE (2010) Beyond the Factor of Safety: Developing Fragility Curves to Characterize System Reliability. Geotechnical and Structures Laboratory, Washington, DC, USA, SR-10-1.

Uzielli M, Lacasse S, Nadim F and Phoon KK (2006) Soil variability analysis for geotechnical practice. In Characterization and Engineering Properties of Natural Soils (Tan TS, Phoon KK, Hight DW and Leroueil S (eds)). Taylor & Francis, London, UK, vol. 3, pp. 1653–1752.

Vick SG (2002) Degrees of Belief: Subjective Probability and Engineering Judgment. ASCE, Reston, VA, USA.

Zhang Y and Der Kiureghian A (1995) Two improved algorithms for reliability analysis. In Reliability and Optimization of Structural Systems: Proceedings of the Sixth IFIP WG7.5 Working Conference on Reliability and Optimization of Structural Systems 1994 (Rackwitz R, Augusti G and Borri A (eds)). Springer, Boston, MA, USA, pp. 297–304.